

*Short Communication*

## **Electrochemical Impedance Spectroscopy Study on Hydration Feature of Calcium Sulfoaluminate Cements**

Qiancheng Fang, Shang Li\*

Institute of Architecture Engineering, Huanghuai University, 463000, China

\*E-mail: [fangqiancheng314@yeah.net](mailto:fangqiancheng314@yeah.net)

Received: 2 February 2019 / Accepted: 5 April 2019 / Published: 10 May 2019

---

Electrochemical impedance spectroscopy (EIS) was used to study the hydration procedure of calcium sulfoaluminate (CSA) cements as a nondestructive testing method. The CSA cements were prepared by mixing the CSA clinker with commercial micronized natural gypsum. The compressive strength evolution of mortars prepared from gypsum pastes indicates that the results are in perfect agreement with the formation of the ettringite. The experimental results indicate that the EIS behavior of CSA cements was varied with the hydration process and increasing hydration time, as the resistance of ion transport processes ( $R_{CT}$ ) gradually increased. Furthermore, the  $R_{CT}$  and semicircle Nyquist curve in high-frequency reduces gradually by increasing the water cement ratio. The curve of impedance spectrum move to the right by increasing gypsum content in cement paste resulting in the increase of  $R_{CT1}$  with gypsum concentration increasing. The experimental findings show that EIS method is an appropriate technique for evaluation of the hydration feature of CSA cements.

---

**Keywords:** Calcium sulfoaluminate cements; Electrochemical impedance spectroscopy; Gypsum contents; Water cement (w/c) ratio; Hydration process

### **1. INTRODUCTION**

The desire to produce sustainable cement development has led to an increase in research activities on calcium sulfoaluminate (CSA) over the past few decades [1-3]. CSA cements are introduced as a very interesting hydraulic binders to achieve both durability and sustainability. The CSA cement production releases less  $CO_2$  into environment relative to Portland cement (PC) [4, 5]. Indeed, the furnace temperature required to produce a CSA clinker is about 1250 °C, which is lower than the used temperature for PC clinker [6]. Furthermore, the low demand of limestone for the production of CSA cement decreases its carbon footprint [7, 8]. The intrinsic porous property of CSA clinker makes it easily grindable which leads to an improvement in energy saving [9].

The initial hydration of CSA cement materials is principally follows the reactivity and the amount of the calcium sulfate added [10, 11] which creates major crystalline phases monosulfate and ettringite [12]. Moreover, the hydration heat is completely released through the first day of hydration [13]. The water cement (w/c) ratio needed for complete hydration in the CSA cements is higher than an ordinary Portland cement (OPC). For example, pure Ye'elinite reacted with an amount of anhydrite to produce ettringite needs a w/c ratio of 0.78 which can produce pastes with pore diameters larger than OPC pastes [14]. Furthermore, both low and high w/c ratios might include extensive development with high w/c ratios and also lead to strength development problems [15]; however, the use of additives with lower particle size can eliminate some of these unfavorable properties [16].

Some researchers control the released heat during the cement hydration by calorimetric testing [17, 18]. However, this method is not able to provide continuous testing due to the damage of the specimens after testing. Some nondestructive techniques are used to evaluate the hydration of cement pastes, such as electrical resistivity method and active acoustic method [19, 20]. In this study, a low-cost, convenient and highly-sensitive electrochemical impedance spectroscopy (EIS) technique as a nondestructive stable-state method is used [21]. The EIS can be used to investigate the microstructure development that happened during the cement hydration; since cement pastes can be studied as an electrochemical system, its hydration is a complex electrochemical method that includes the transfer, distribution and rearrangement of ions. Consequently, EIS technique can be used to consider the hydration process of mixed cement materials [22].

Although many studies have been reported on hydration of CSA cement, studies related to EIS measurements of CSA cement materials are still limited. In this study, the effect of various parameters on the hydration of cement pastes such as the w/c ratio and the amount of gypsum were investigated. This research was performed by the study of the mechanical properties and hydration process of relevant mortars. Using the optimal amount and the type of additives increase the cement efficiency, resulting in a lower w/c ratio to obtain higher compressive strength.

## 2. MATERIALS AND METHOD:

**Table 1.** The composition of the CSA clinker

Compositions	Concentration (wt.%)
Calcium oxide (CaO)	41.2
Silica (SiO <sub>2</sub> )	6.9
Alumina (Al <sub>2</sub> O <sub>3</sub> )	26.8
Iron oxide (Fe <sub>2</sub> O <sub>3</sub> )	0.88
Magnesium oxide (MgO)	0.75
Sulfur trioxide (SO <sub>3</sub> )	19.5
Titanium dioxide (TiO <sub>2</sub> )	1.2
Sodium oxide (Na <sub>2</sub> O)	0.13
Potassium oxide (K <sub>2</sub> O)	0.40
Loss on ignition (LoI)	1.8

A commercial calcium sulphoaluminate (CSA) clinker and natural gypsum are used industrially as raw materials which are produced and marketed in China. The composition of the CSA clinker is summarized in Table 1. CSA cements were produced by mixing the CSA clinker with the appropriate amount of natural gypsum in 10, 15 and 20 wt.% for a duration of 15 min.

The Blaine fineness values defined for gypsum and CSA were 500 and 480 m<sup>2</sup>/kg, respectively. Thus, all blended samples exhibited Blaine values close to 480 m<sup>2</sup>/kg.

Cement pastes were produced with water and CSA cement (w/c) ratios of 0.35, 0.45 and 0.55. A polycarboxylate-based superplasticizer was added into the concrete mixture with a 25 wt.%.

The cement paste materials were mechanically stirred by helices according to a standard procedure. Ultimate compressive strengths of 40\*40\*160 mm<sup>3</sup> samples were determined according to a compression testing mechanism (YAW-300B) at 0.125, 1, 7, and 28 days.

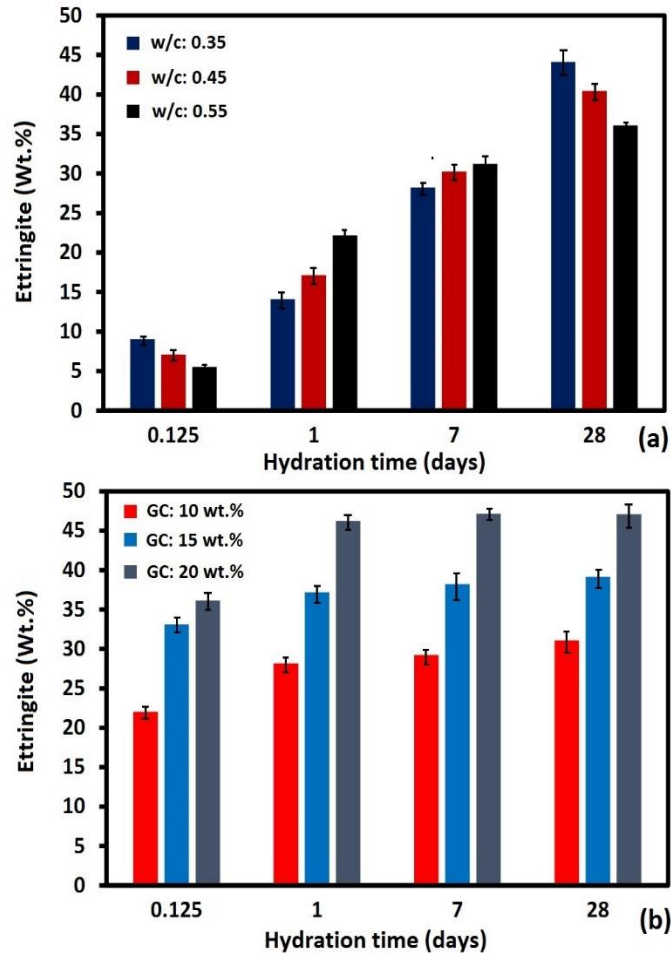
The EIS system was applied to study electrochemically analysis of the samples at ambient temperature range for the mixed cements with different hydration times (0.125, 1, 7, and 28 days). To create a good contact between the specimen and the electrode, a thin and wet sponge was utilized and was inserted into the gap between them. The tests were done using an impedance gain phase analyzer (Solartron-Si1287/Si1260). The ZView program was used to investigate the EIS spectrum of the cement system.

Laboratory X-Ray Powder Diffraction (LXRPD) patterns of all samples were investigated by the Rietveld technique using the GSAS software package to achieve the Rietveld quantitative phase analysis (RQPA). The Amorphous and Crystalline non-quantified contents were considered through external standard technique (G-factor) from LXRPD in reflection mode data. Compressive strengths of the specimens were calculated at 0.125, 1, 7, and 28 days in a compression press (Model Autotest 200/10 W, Ibertest) according to EN196-1 and at a rate of 1.5 MPa/s. The surface morphology of the samples were characterized by scanning electron microscopy (SEM; FEI/Nova NanoSEM 450).

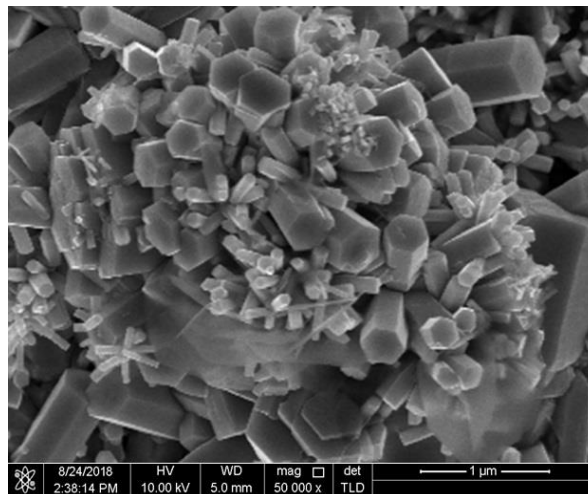
### 3. RESULTS AND DISCUSSION

Figure 1 indicates ettringite concentrations for the four hydrating systems in various conditions, taken from RQPA results.

Fig. 1a shows the ettringite contents as a function of hydration time for different water cement ratio. For 0.55 w/c pastes at hydration time of 3h, gypsum pastes reveal the lowest ettringite concentrations which can be attributed to the low rate of dissolution of gypsum when compared to other w/c ratios. However, crystallization of AFt at 0.55 w/c ratio is higher at hydration periods higher than 24 h. Ettringite crystallization is slightly affected when using the water concentration in gypsum pastes. Though, AFt crystallizes at a slower pace in gypsum pastes by increasing the w/c ratios at hydration periods higher than 7 days. As shown in figure 1b, the highest ettringite amounts are formed by increasing the concentration of gypsum. On the other hand, the compressive strength evolution of mortars prepared from gypsum pastes indicates that the results are in perfect agreement with the formation of the ettringite [23].



**Figure 1.** The ettringite contents as a function of hydration time for (a) different water cement ratio in a constant gypsum content (20 wt.%) and (b) different concentration of gypsum in a constant w/c ratio (0.45)



**Figure 2.** SEM image of hydrated CSA cement with gypsum concentration of 20 wt.% at 1 day of hydration time

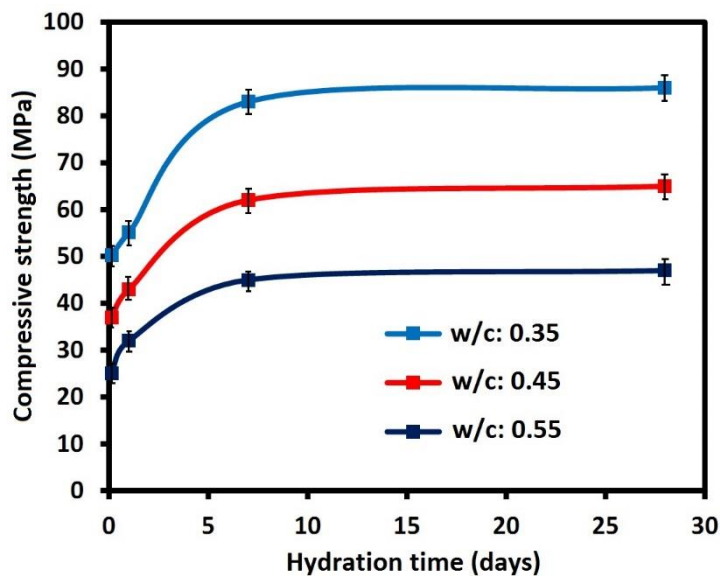


**Figure 3.** Compressive strength of mortars according to various w/c ratio (0.35, 0.45 and 0.55) in a constant gypsum content (20 wt.%).

In Figure 2, SEM image for hydrated CSA cement with gypsum concentration of 20 wt.% is reported at 1 day of hydration time. During the hydration periods, ettringite structures take the shape of hexagonal crystals in a cross section view; where their size can vary considerably. As shown in figure 2, extremely large ettringite crystals formed in CSA cements with 0.1–0.5  $\mu\text{m}$  wide and about 0.4–1.5  $\mu\text{m}$  long.

The mechanical properties of the specimens were also studied. Figure 3 indicates the values of compressive strength of mortars according to various w/c ratio in a constant gypsum content. They were performed on small cubes as defined in the experimental section. It is clear from the data analysis that the mortar with 0.35 w/c ratio has a higher mechanical performance than the others. Reactions in gypsum pastes occur rapidly, and their low setting time is extremely sensitive to the homogeneous degree of the mortars. Adding a small amount of gypsum improves the mortar's performance, but does not significantly delay the reaction until the setting time, so the mortar indicates low values of mechanical force, and slightly higher when the gypsum is added [24].

The impedance spectroscopy parameters can well reflected some microstructure characteristics of concrete material [25, 26]. For instance, the electrical resistance of an electrolyte ( $R_{\Omega}$ ) in a pore solution may be attained using the intersection of the high frequency side semicircle in the Nyquist diagram to the real axis.  $R_{\Omega}$  indicates the characteristics of the concrete porosity and pore solution, i.e., the larger the  $R_{\Omega}$ , the smaller the value of the concrete porosity. The diameter of the high frequency semicircle ( $R_{CT}$ ) in Nyquist diagram, indicates the polarization resistance during the charge transfer of hydrated electrons. Investigations have shown that  $R_{CT}$  indicates the hydration degree of cement paste [27]. Furthermore,  $R_{CT}$  indirectly reveals the concentration of  $\text{OH}^-$  ions.

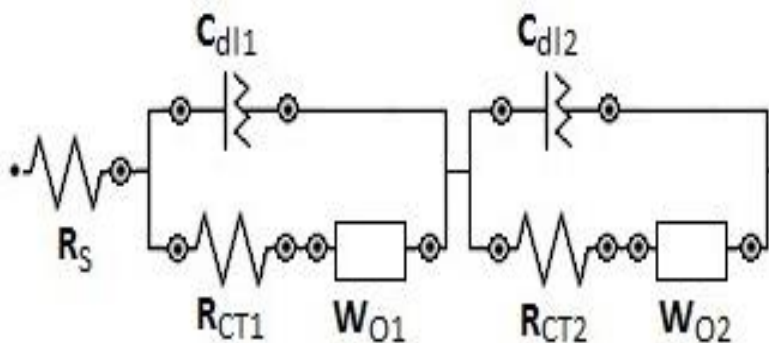


**Figure 4.** The equivalent electrochemical circuit

Figure 4 shows an electrical circuit model for investigation of mortar’s hydration. According to hydration process,  $R_{CT1}$  is resistance procedure to ion transfer in cement interior structure that is inversely proportional to hydrated electrons in the internal structure of cement and hydroxide ion concentration of the cement pore solution [28, 29]. Figure 5 exhibits the Nyquist plot of cement paste with different w/c ratio. It is obtained through the curves that is form by the decreasing semicircle radius at high-frequency with an increasing w/c ratio. In other words, the  $R_{CT1}$  increases with a reducing w/c ratio. The reason is that the smaller the w/c ratio, the less the internal solution and as a result, the ion content is reducing in the internal structure of the cement paste.

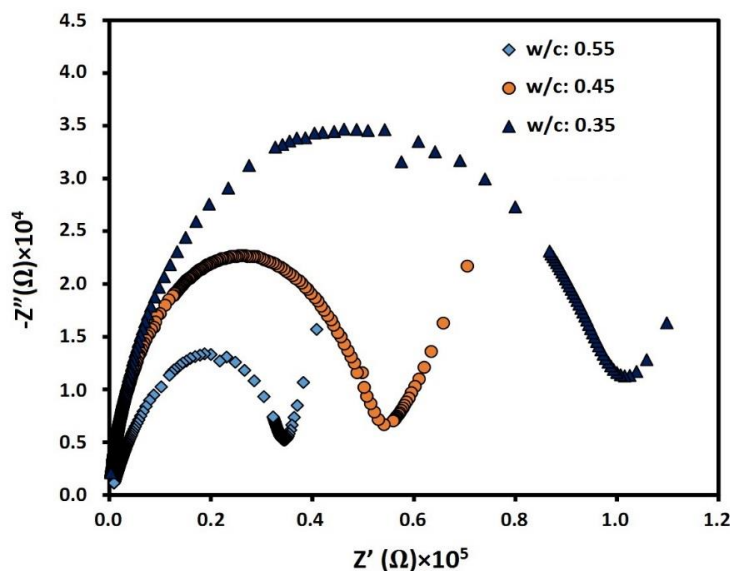


**Figure 5.** Nyquist plots of cement paste with different w/c ratio in a constant gypsum content (20 wt.%) at hydration time of 7 days

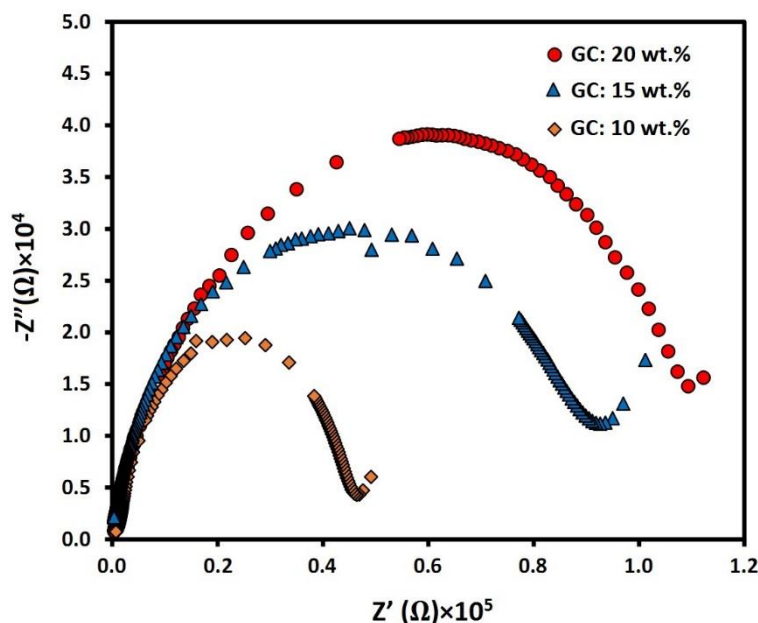


**Figure 6.** Nyquist plots of cement paste with different gypsum contents in a constant w/c ratio (0.45) at hydration time of 7 days

The Nyquist plots with different gypsum contents is shown in Figure 6. The curve of impedance spectrum move to the right with the increase of gypsum content in the cement paste resulting in an increase of R<sub>CT1</sub> with the increase of gypsum concentration [30]. Figure 7 indicates the R<sub>CT1</sub> variation for different hydration periods in different gypsum content of identical w/c ratio.

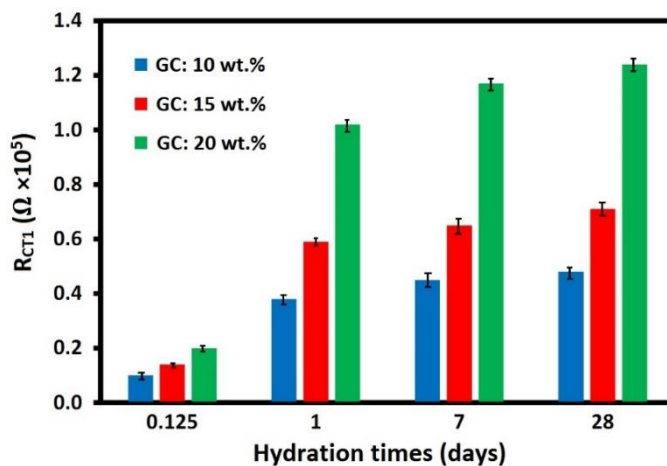


**Figure 7.** The R<sub>CT1</sub> variation with hydration period in different gypsum content (10, 15 and 20 wt.%) of identical w/c ratio (0.45)

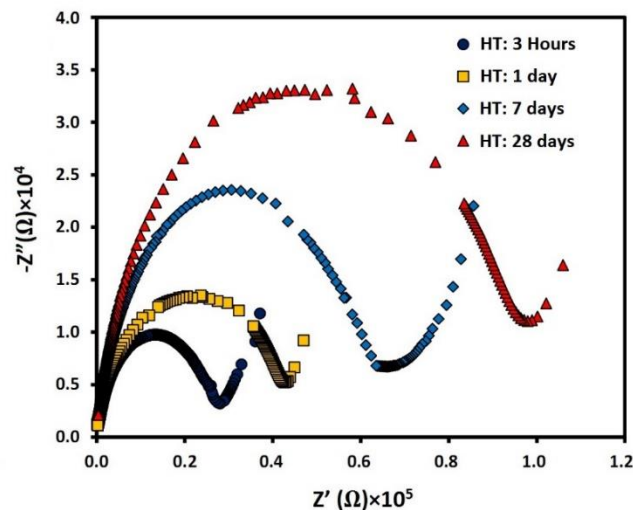


**Figure 8.** electrochemical impedance spectroscopy evaluation on hydration process of CSA cements in a constant w/c ratio (0.45) and 20 wt.% gypsum content

Since  $R_{CT1}$  of 20 wt.% gypsum content has the highest amounts among the other curves, and 10 wt.% gypsum content lies at the more inferior location. Thus,  $R_{CT1}$  grows with the increase of gypsum concentration. Figure 8 shows electrochemical impedance spectroscopy evaluation on hydration process of CSA cements. As shown in Figure 8, a semicircle gradually increased in the early stages. By increasing the hydration period, the semicircle gradually increases. The low frequency region had a straight line with a gradient angle of  $45^\circ$  for all the curves.

#### 4. CONCLUSIONS

The CSA cement hydration was considered by varying the w/c ratio and gypsum concentrations of the cement materials. Hydration process was significantly accelerated via the presence of gypsum. The compressive strength evolution of mortars prepared from gypsum pastes indicates that the results are in perfect agreement with the formation of the ettringite. The data analysis indicate that the mortar with 0.35 w/c ratio has a higher mechanical performance than the others. Nyquist plots of cement paste show that the semicircles radii decrease at high-frequency with increasing w/c ratio. The  $R_{CT1}$  variation with hydration periods in different gypsum content indicated an increase by increasing the gypsum concentration.

#### References

1. J. Bizzozero, C. Gosselin and K.L. Scrivener, *Cem. Concr. Res.*, 56 (2014) 190.
2. N. Khalil, G. Aouad, K. El Cheikh and S. Rémond, *Constr. Build. Mater.*, 157 (2017) 382.
3. Y. Shen, X. Chen, W. Zhang, X. Li and J. Qian, *Constr. Build. Mater.*, 193 (2018) 221.
4. K.L. Scrivener, V.M. John and E.M. Gartner, *Cement Concrete Res.*, 114 (2018) 2.

5. S. Kakooei, H.M. Akil, A. Dolati and J. Rouhi, *Constr. Build. Mater.*, 35 (2012) 564.
6. A. Viani and A.F. Gualtieri, *J. Hazard. Mater.*, 260 (2013) 813.
7. G.R. de Sensale and I.R. Viacava, *Constr. Build. Mater.*, 166 (2018) 873.
8. R. Puente-Ornelas, L.C. Guerrero, G. Fajardo-San Miguel, E. Rodríguez, A. Trujillo-Álvarez, H. Rivas-Lozano and H. Delgadillo-Guerra, *Int. J. Electrochem. Sc.*, 11 (2016) 277.
9. E. Gartner and T. Sui, *Cem. Concr. Res.*, 114 (2018) 27.
10. R. Trauchessec, J.-M. Mechling, A. Lecomte, A. Roux and B. Le Rolland, *Cem. Concr. Compos.*, 56 (2015) 106.
11. Y. Jeong, C. Hargis, S. Chun and J. Moon, *Materials*, 10 (2017) 900.
12. W. Frank and L. Barbara, *Cem. Concr. Res.*, 40 (2010) 1239.
13. M. García-Maté, G. Angeles, L. León-Reina, E.R. Losilla, M.A. Aranda and I. Santacruz, *Cem. Concr. Compos.*, 55 (2015) 53.
14. G. Bernardo, A. Telesca and G.L. Valenti, *Cem. Concr. Res.*, 36 (2006) 1042.
15. J. Ambroise, J. Georgin, S. Peysson and J. Péra, *Cem. Concr. Compos.*, 31 (2009) 474.
16. W. Chang, H. Li, M. Wei, Z. Zhu, J. Zhang and M. Pei, *Mater. Res. Innovations*, 13 (2009) 7.
17. V. Tydlitát, T. Matas and R. Černý, *Constr. Build. Mater.*, 50 (2014) 140.
18. X. Pang, D.P. Bentz, C. Meyer, G.P. Funkhouser and R. Darbe, *Cem. Concr. Compos.*, 39 (2013) 23.
19. Y. Lu, H. Ma and Z. Li, *J. Intell. Mater. Syst. Struct.*, 26 (2015) 280.
20. B. Dong, J. Zhang, Y. Wang, G. Fang, Y. Liu and F. Xing, *Constr. Build. Mater.*, 119 (2016) 16.
21. C. Pan, J. Geng and Q. Ding, *Int. J. Electrochem. Sc.*, 13 (2018) 6098.
22. W. Aperador, J. Duque and E. Delgado, *Int. J. Electrochem. Sc.*, 11 (2016) 3755.
23. H. Nguyen, E. Adesanya, K. Ohenoja, L. Kriskova, Y. Pontikes, P. Kinnunen and M. Illikainen, *Constr. Build. Mater.*, 197 (2019) 143.
24. S. Cunha, J.B. Aguiar and A. Tadeu, *Constr. Build. Mater.*, 122 (2016) 637.
25. P. Gu, P. Xie, J.J. Beaudoin and R. Brousseau, *Cem. Concr. Res.*, 22 (1992) 833.
26. B.J. Christensen, T. Coverdale, R.A. Olson, S.J. Ford, E.J. Garboczi, H.M. Jennings and T.O. Mason, *J. Am. Ceram. Soc.*, 77 (1994) 2789.
27. M. Shi, Z. Chen and J. Sun, *Cement and Concrete Research*, 29 (1999) 1111.
28. K.A. Snyder, X. Feng, B. Keen and T. Mason, *Cem. Concr. Res.*, 33 (2003) 793.
29. Q. Qiu, Z. Gu, J. Xiang, C. Huang and B. Dong, *ACI Mater. J.*, 114 (2017) 605.
30. C. Ma, Y. Bu and B. Chen, *Constr. Build. Mater.*, 60 (2014) 25.